Cent. Eur. J. Phys. • 8(5) • 2010 • 746-759
DOI: 10.2478/s11534-010-0001-4

VERSITA

Central European Journal of **Physics**

Calculation of atomic spontaneous emission rate in 1D finite photonic crystal with defects

Research Article

Adam Rudziński[1]*, Paweł Szczepański[1,2]

1 *Institute of Microelectronics and Optoelectronics, Warsaw University of Technology, ul. Koszykowa 75, 00-665 Warszawa, Poland*

2 *National Institute of Telecommunications, ul. Szachowa 1, 00-894 Warszawa, Poland*

Received 4 October 2009; accepted 9 December 2009

Abstract: We derive an expression for the spontaneous-emission rate in finite one-dimensional photonic crystals with arbitrary defects, using the effective resonator model to describe electromagnetic field distributions in the structure. We obtain explicit formulae for contributions from different modes, *i.e.* radiation, substrate and guided modes. Formal calculations are illustrated by a few numerical examples, which demonstrate that application of the effective resonator model simplifies the interpretation of results.

PACS (2008): 42.50.Ct, 42.50.Pq, 42.70.Qs

Keywords: photonic crystal • multi-layer waveguide • spontaneous emission • defects • effective resonator model

1. Introduction

It is a long known fact that the interaction of a system with electromagnetic radiation is affected not only by the system itself, but also by the environment in which it is situated. Placement of an atom or a molecule in a cavity leads to many effects not present in an unbounded vacuum, which are the subject of studies within the area of so-called cavity QED – for a review see e.g. [1]. In particular, one phenomenon is the modification of the spontaneous emission rate, predicted by Purcell [2] and later verified in many experiments, e.g. [3–6]. This fact has considerable consequences for contemporary science and technology, therefore it is an important object of research. Because spontaneous emission is a quantum effect, it is necessary to employ a formalism based on quantization of the electromagnetic field when modelling it. A theoretical description suitable for the treatment of spontaneous emission in dielectric structures, followed in many papers, has been discussed by Glauber and Lewenstein [7].

Another fact, recognized over a hundred years ago and described by Lord Rayleigh [8], is that a periodically arranged medium has peculiar properties, with the most interesting being the existence of band gaps – frequency ranges in which no propagating waves exist. In photonics, periodic dielectric materials with band gaps for electromagnetic waves (photonic band gaps) are called photonic crystals. The simplest of these structures are one-dimensional photonic crystals, built of alternating layers with two different refractive indices and widths (which

*E-mail: arudzins@poczta.onet.pl

can, in fact, be considered a particular type of planar multi-layer waveguide). Such photonic crystals are a particularly good subject of study, because one-dimensional multi-layers can be described analytically and are significant from the practical point of view. With proper choice of parameters, it is possible to obtain a band gap for all directions of propagation, as has been previously shown [9–11]. Even without a full band gap, a one-dimensional periodic lattice allows for significant modification of light emission, and therefore it is useful for the construction of devices such as light emitting diodes or lasers [6, 12, 13]. To understand their operation, and to be able to design them with care for various details, it is important to properly describe the impact of the structure on the light-emission process.

A perfect photonic crystal, which is strictly a periodic structure, consists of an infinite number of elementary cells (*i.e.* groups of layers, which appear in the same sequence in every period) and can be modeled using the Floquet-Bloch theorem, fixing the form of modes of the structure. A recent example of this treatment is [14], in which spontaneous emission has been described with a classically derived formula. A practical realization of a photonic crystal is inevitably of finite size, thus in more realistic models the structure must be treated rather as a planar multi-layer waveguide. This approach also makes it possible to account for defects (of width or refractive index) in the structure. Just as in a perfect photonic crystal, it is possible to use a classical description of spontaneous emission in a planar waveguide, e.g. [15]. One has to note, though, that what is actually calculated this way is radiation of a classical electric dipole; only comparison with a result from quantum theory allows us to establish its relation to spontaneous emission. Hence, such treatment is just a limited reconstruction of a specific formula, and not a relevant, general theory in any way. A proper, versatile description of spontaneous emission has to be established in the quantum framework, like [7]. For a multi-layer waveguide, a particular case of which is a finite one-dimensional photonic crystal, one cannot use the Floquet-Bloch theorem and has to choose modes of the structure in a different way. A basis suitable for a single interface between two media has been proposed by Carniglia and Mandel [16]. In their proposition, the set of modes is constructed starting with plane waves propagating towards the structure (sweeping through all frequencies and angles of incidence), thus it can be referred to as a set of so-called incoming modes. Each incident plane wave has to be accompanied by respective reflected and transmitted waves, and such a triplet constitutes a field distribution in the structure. Modes of this form are particularly simple and form orthogonal [17] and complete [18] set. A modification of this model also exists, in which instead of waves propagating *towards* the interface, waves propagating *away* from the interface are used [19], so-called outgoing modes. With this choice there is always only one emitted plane wave carrying power out in a chosen direction, and this set is considered favorable for these kinds of calculations, e.g. in [20]. For a multi-layer structure, it is necessary to supplement these models with guided modes, calculated for the layer with the highest refractive index [21]. Radiation modes can be redefined as combinations of incoming or outgoing modes, for which no power flow in the transverse direction occurs, assuring their orthogonality [22]. Field distributions of modes can be conveniently found with the help of the translation matrix method [23, 24].

A common feature of these models is an external radiation source exciting a mode, which seems not to be particularly suitable for description of emission from a system located inside the structure because it leads to treatment of the structure as a whole block, instead of distinguishing particular locations inside, which may have significantly different properties.

However, it *is* possible to find field distributions starting from a plane wave emerging in one of the layers. This approach, described or employed e.g. in [25, 26], requires summing up of all the reflected waves appearing in the layer, which resembles a text-book exercise of calculating transmission through a FP resonator. The difference is that in the case of a source *inside* the layer, reflections occur at both interfaces, thus there are twice as many waves to sum. Modes obtained with this method are indexed by wave vectors and polarizations, and naturally split into radiation, substrate and guided modes. This construction of modes is also the starting point of the effective resonator model [27–31], which allows a very clear physical interpretation of obtained results. The model is not just limited to calculating electromagnetic field distributions; its main advantage is the definition of a quantity called the *mode spectrum*, which can be used to quickly and conveniently analyze modes and properties of the structure. Assuming, that the interfaces between layers are perpendicular to the z axis, the mode spectrum of a specific layer is defined as

$$\rho_{\epsilon}(\boldsymbol{k}) = \frac{1}{8\pi^3} \frac{1 - |r_L r_R|^2}{|1 - r_L r_R \exp(2\mathrm{i} k_z L_z)|^2}, \tag{1}$$

where $\boldsymbol{k}$ is a wave vector and ϵ – represents polarization of the mode, r_L and r_R are reflection coefficients for the stacks of layers on each side of the source layer (*i.e.* subscript L indicates "left" and R for "right"; these coefficients are functions of polarization and wave vector, but for clarity of the expression this is not explicitly denoted),

k_z is the z component of the wave vector and L_z is the layer's width. Similar expressions have already appeared in the literature, but they have never been given such an important physical meaning. The mode spectrum is a quantity directly related to both the density of states and the spontaneous emission rate, resembling the quality factor of a cavity, which also takes into account interference between plane waves comprising a mode. If the quality factor for a mode is high, then the value of the mode spectrum is high (when the interference is constructive), or low (if the interference is destructive). In particular, if the mode spectrum is equal to zero, this means, that the field of the mode is completely extinguished in the cavity. For modes for which the quality factor is low, the value of the mode spectrum is close to the free-space value

$$\rho^{\mathrm{fs}} = \frac{1}{8\pi^3}. \tag{2}$$

In this paper, we derive an expression for the spontaneous-emission rate in a one-dimensional photonic crystal with arbitrary defects of width or refractive index in any layers, split into explicit contributions from different modes, *i.e.* radiation, substrate and guided modes, obtained with the help of the effective resonator model. It is shown that the mode spectrum characterizes the spontaneous emission rates inherent to each layer. It allows for an easy investigation of properties of the structure, in particular containing defects, either introduced intentionally [32] or random fabrication impurities, which have negative influence on the structure [33]. Calculations conducted with the effective resonator model lead to a description of spontaneous emission which is particularly convenient for research on the impact of structure on the process, or for dealing with practical tasks where a proper design for the structure is necessary. Obtained results can be used for detailed studies of how a multi-layer environment affects spontaneous emission decay; firstly to identify the modes which contribute most in particular layers –a process which is not straightforward with different mode constructions. The effective resonator model is completely analytic, thus, in principle, it allows us to obtain analytic expressions describing various aspects of the phenomenon, or it could be used as the basis for semi-analytic or approximate calculations in more complicated structures. The rest of this paper is organized as follows: In Sec. 2, we define the considered structure, introduce dimensionless parameters, particularly suitable for analysis of its properties, and briefly review a few properties of modes in the effective resonator model. Next, in Sec. 3, we describe the quantum formalism adopted for calculations, which we employ in Sec. 4 to obtain the expression for spontaneous emission rate. Contributions from different kinds of modes are the subject of calculations in Sec. 5. We provide a few exemplary results in Sec. 6, while Sec. 7 summarizes the paper.

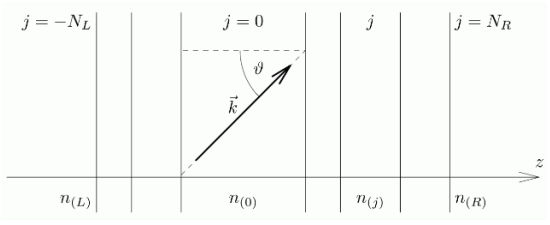

Figure 1. Sketched structure of dielectric multi-layer waveguide.

2. Considered structure and adopted notation

We consider the structure of a finite one-dimensional photonic crystal, which is a particular case of a dielectric multi-layer waveguide, as sketched in Fig. 1. We define the z axis perpendicular to interfaces between dielectric layers, which we assume to be made of lossless, isotropic dielectrics. The refractive index of the structure is then given by

$$n(\boldsymbol{r}) = \sum_j \chi_j(z)\, n_{(j)}, \tag{3}$$

where j indexes layers, $n_{(j)}$ is the refractive index of the jth layer, and $\chi_j(z)$ the characteristic function of the jth layer: $\chi_j(z) = 1$ for z in the jth layer and $\chi_j(z) = 0$ for z from outside of it. Index j runs from $-N_L \leq 0$ to $N_R \geq 0$ and we put $z = 0$ at the left boundary of the layer for which we choose $j = 0$. We treat the media outside as layers with $j = -N_L$ and $j = N_R$, but additionally assume that $n_{(R)} \leq n_{(L)}$ (in subscripts and superscripts we use abbreviations $R \equiv N_R$ and $L \equiv -N_L$) – this is just a matter of the z axis orientation, therefore it does not affect generality of the model or the presented calculations. We denote the width of the jth layer by $L_z^{(j)}$, using $L_z \equiv L_z^{(0)}$ for the $j = 0$ layer, and we assume that layers extend to infinity in the x and y directions. For our one-dimensional photonic crystal:

$$n_{(j)} = \begin{cases} n_1 & \text{for even } j, \\ n_2 & \text{for odd } j, \end{cases} \tag{4a}$$

and

$$L_z^{(j)} = \begin{cases} L_1 & \text{for even } j, \\ L_2 & \text{for odd } j, \end{cases} \tag{4b}$$

except for defected layers and the surrounding media, for which the general notation $n_{(j)}$ and $L_z^{(j)}$ will be kept.

Modes of the structure are indexed with the wave vector $\boldsymbol{k}$ and polarization $\epsilon = \mathrm{TE}, \mathrm{TM}$. Electric and magnetic field distributions are bound to each of them, represented by $\boldsymbol{f}_{k\epsilon}(\boldsymbol{r})$ and $\boldsymbol{f}^H_{k\epsilon}(\boldsymbol{r})$. Different layers are equipped with different sets of modes, in this paper we always refer to modes of the layer with $j = 0$, thus we obtain results relevant for this particular layer (but chosen arbitrarily). Construction of these modes is discussed with details in [28–31], here we wish to briefly review only a few of their properties.

Electric and magnetic fields radiated by a source inside the $j = 0$ layer can be written in terms of field distributions $\boldsymbol{f}_{k\epsilon}$ and $\boldsymbol{f}^H_{k\epsilon}$:

$$\begin{aligned}\boldsymbol{E}(\boldsymbol{r},t) &= \iint\!\!\!\sum_{\boldsymbol{k},\epsilon} \mathcal{E}_{k\epsilon}(t)\,\boldsymbol{f}_{k\epsilon}(\boldsymbol{r}) \qquad (5a)\\ &\equiv \sum_{\epsilon}\int_{\mathrm{RSM}} \mathrm{d}^3k\,\mathcal{E}_{k\epsilon}(t)\,\boldsymbol{f}_{k\epsilon}(\boldsymbol{r})\\ &\quad + \sum_{\epsilon}\int \mathrm{d}^2k_{\parallel} \sum_{a\in \mathrm{GM}\left(k_{\parallel},\epsilon\right)} \mathcal{E}_{k_a\epsilon}(t)\,\boldsymbol{f}_{k_a\epsilon}(\boldsymbol{r})\,,\\ \boldsymbol{H}(\boldsymbol{r},t) &= \iint\!\!\!\sum_{\boldsymbol{k},\epsilon} \mathcal{B}_{k\epsilon}(t)\,\boldsymbol{f}^H_{k\epsilon}(\boldsymbol{r})\,, \qquad (5b)\end{aligned}$$

where $\mathcal{E}_{k\epsilon}(t)$ and $\mathcal{B}_{k\epsilon}(t)$ are time-dependent amplitudes, RSM denotes a subset of radiation and substrate modes, and $\mathrm{GM}\left(k_{\parallel},\epsilon\right)$ – discrete subset of guided modes with given $k_{\parallel} \equiv \sqrt{k_x^2 + k_y^2}$ and polarization ϵ. For guided modes the integration is performed over components k_x and k_y, while the whole wave vector of the ath guided mode is $\boldsymbol{k}_a \equiv k_x\boldsymbol{e}_x + k_y\boldsymbol{e}_y + k_{z,a}\boldsymbol{e}_z$. Decomposition of modes into radiation, substrate and guided modes is based on a standard criterion of total reflection, we precisely define each of these subsets in Sec. 5. To improve clarity, we use the "sum-integral" symbol, which combines integration over the components of the wave vector, and summation over discrete guided modes – expression (5a) can be considered its definition.

Every mode can be identified with its electric field distribution, because magnetic field distributions can be obtained from the relation:

$$\boldsymbol{f}^H_{k\epsilon} = \frac{\nabla \times \boldsymbol{f}_{k\epsilon}}{\mathrm{i}\mu_0\omega_k}, \qquad (6)$$

where

$$\omega_k = \frac{c}{n_{(0)}}\sqrt{\boldsymbol{k}^2} \qquad (7)$$

is the angular frequency of the mode. The last expression is the well known dispersion relation for a plane wave, which is a condition the plane wave must satisfy to be a valid mathematical solution of Maxwell's equations, in which ω_k and the components of $\boldsymbol{k}$ can be complex numbers in general. Further restrictions can be settled by a requirement that the field must be physical, *i.e.* must not "explode" in infinity, meaning that the exponents $\exp(\mathrm{i}\boldsymbol{k}\cdot\boldsymbol{r})\exp(-\mathrm{i}\omega_k t)$ should either oscillate or fade. An obvious notion is that $\omega_k \in \mathbb{R}$, because of the time uniformity, similarly $k_x, k_y \in \mathbb{R}$, because the considered structure is uniform in the x and y directions, but spatial dependence in the z direction is more complicated. The field is always physical if $k_z \in \mathbb{R}$, but in general this can be true for some imaginary values $k_z \in \mathrm{i}\mathbb{R}$, if the refractive index of the layer is sufficiently small (the field has to be oscillatory in another layer in order to connect two evanescent waves fading in opposite directions). However, in this paper we wish to concentrate only on modes with real wave vectors $\boldsymbol{k} \in \mathbb{R}^3$, *i.e.* our considerations are limited to layers with sufficiently high refractive index. The reason is that for a single non-uniform plane wave with imaginary k_z there is no flow of energy in the z direction, thus, a natural choice of waves on an interface between two layers does not contain a reflected wave. As our definition of the mode spectrum is based on reflection coefficients, it cannot be naturally applied for non-uniform plane waves, and we wish to show in this paper that this quantity is important for spontaneous emission. Therefore, from now on we will assume $k_z \in \mathbb{R}$.

Modes $\boldsymbol{f}_{k\epsilon}$ are orthonormal, and their orthonormalization rules are:

$$\int \mathrm{d}^3r\,\varepsilon(\boldsymbol{r})\,\boldsymbol{f}^*_{q\lambda}(\boldsymbol{r})\cdot\boldsymbol{f}_{k\epsilon}(\boldsymbol{r}) = \delta_{\epsilon\lambda}\delta(\boldsymbol{k}-\boldsymbol{q})\,, \qquad (8a)$$

for radiation and substrate modes, while for guided modes:

$$\int \mathrm{d}^3r\,\varepsilon(\boldsymbol{r})\,\boldsymbol{f}^*_{q_b\lambda}(\boldsymbol{r})\cdot\boldsymbol{f}_{k_a\epsilon}(\boldsymbol{r}) = \delta_{\epsilon\lambda}\delta(k_x-q_x)\,\delta\left(k_y-q_y\right)\,\delta_{ab}. \qquad (8b)$$

In the considered case, the relative electric permittivity $\varepsilon(\boldsymbol{r}) = n^2(\boldsymbol{r})$. Modes $\boldsymbol{f}_{k\epsilon}$ can be used to represent the generalized transverse delta function $\delta^{ij}_{\varepsilon\perp}(\boldsymbol{r},\boldsymbol{r}')$, which is a tensor conserving transverse fields. It is defined by the relation [7]

$$\int \mathrm{d}^3r'\,\varepsilon\left(\boldsymbol{r}'\right)\,\delta^{ij}_{\varepsilon\perp}\left(\boldsymbol{r},\boldsymbol{r}'\right)\,f^j_{k\epsilon}\left(\boldsymbol{r}'\right) = f^i_{k\epsilon}(\boldsymbol{r}) \qquad (9)$$

(in this, and the remaining expressions in the paper, we use the summation convention for upper indices). The generalized transverse delta can then be represented as:

$$\delta^{ij}_{\varepsilon\perp}\left(\boldsymbol{r},\boldsymbol{r}'\right) = \iint\!\!\!\sum_{\boldsymbol{k},\epsilon} f^i_{k\epsilon}(\boldsymbol{r})\,f^{j*}_{k\epsilon}\left(\boldsymbol{r}'\right)\,. \qquad (10)$$

This function has two important properties, it is real:

$$\delta^{ij*}_{\varepsilon\perp}\left(\boldsymbol{r},\boldsymbol{r}'\right) = \delta^{ij}_{\varepsilon\perp}\left(\boldsymbol{r},\boldsymbol{r}'\right) \qquad (11)$$

and

$$\delta^{ij}_{\epsilon\perp}(\boldsymbol{r},\boldsymbol{r}') = \delta^{ji}_{\epsilon\perp}(\boldsymbol{r}',\boldsymbol{r})\,. \tag{12}$$

These identities can be easily proven using the relation $\boldsymbol{f}^*_{k\epsilon} = -\gamma_\epsilon \boldsymbol{f}_{-k\epsilon}$, with

$$\gamma_\epsilon = \begin{cases} 1, & \text{for } \epsilon = \text{TE}, \\ -1, & \text{for } \epsilon = \text{TM}, \end{cases} \tag{13}$$

which is satisfied by all modes, and $s_{k\epsilon}\boldsymbol{f}_{k_*\epsilon} = \boldsymbol{f}_{k\epsilon}$, satisfied by substrate and guided modes, for which coefficient $s_{k\epsilon} = r_R \exp(2\mathrm{i}k_z L_z)$ [31].

An elementary cell of the considered photonic crystal consists of two layers, the first with width L_1 and refractive index n_1, and the second with width L_2 and refractive index n_2. Optical widths of these layers are defined as $\Lambda_1 = n_1 L_1$, $\Lambda_2 = n_2 L_2$; in general, for the jth layer $\Lambda^{(j)} = n_{(j)} L_z^{(j)}$. The optical width of the whole elementary cell is then $\Lambda = \Lambda_1 + \Lambda_2$. It is known that properties of photonic crystals depend on the proportions of the structure, thus, to investigate its properties it is convenient to use parameters which are dimensionless, so we use Λ as a unit of length in the construction of such a set. To describe the structure, we use refractive indices, normalized optical widths Λ_i/Λ (in general $\Lambda^{(j)}/\Lambda$), normalized position in the $j = 0$ layer $\zeta = n_{(0)} z/\Lambda^{(0)}$ and normalized frequency $\Theta = f/f_0$, where $f_0 = c/\Lambda$. To obtain more compact expressions, instead of the angle of incidence ϑ, we use its cosine $\eta = \cos\vartheta$. All expressions of our interest can be written in terms of these parameters, e.g.:

$$k_z z = 2\pi\eta\Theta\zeta\frac{\Lambda^{(0)}}{\Lambda}, \tag{14a}$$

$$k_z^{(j)} L_z^{(j)} = \pm 2\pi\Theta\sqrt{1 - \frac{1-\eta^2}{n^2_{(j)}/n^2_{(0)}}}\,\frac{\Lambda^{(j)}}{\Lambda}, \tag{14b}$$

$$\left|\frac{k_z^{(j)}}{k_z}\right| = \sqrt{\left|1 + \frac{n^2_{(j)}/n^2_{(0)} - 1}{\eta^2}\right|}. \tag{14c}$$

3. Hamiltonian of the system

An electromagnetic field and a quantum system (e.g. an atom) interacting with each other can be described with a hamiltonian consisting of three parts:

$$\hat{H} = \hat{H}_{\text{em}} + \hat{H}_{\text{int}} + \hat{H}_{\text{at}}. \tag{15}$$

$\hat{H}_{\text{em}}$ is the hamiltonian of electromagnetic field in an inhomogeneous dielectric medium [7]:

$$\hat{H}_{\text{em}} = \frac{1}{2}\int \mathrm{d}^3 r\ :\left(\varepsilon_0\varepsilon(\boldsymbol{r})\,\boldsymbol{E}^2(\boldsymbol{r}) + \frac{(\nabla\times\boldsymbol{A}(\boldsymbol{r}))^2}{\mu_0}\right):, \tag{16}$$

where colons denote normal ordering, $\boldsymbol{E}$ and $\boldsymbol{A}$ are electric-field and vector-potential operators respectively. $\hat{H}_{\text{at}}$ is the hamiltonian of the quantum system. Because we are interested in the influence of the structure, we use the simplest possible expression, which for an electronic system, an atom or a molecule, in the infinite nuclear mass approximation (the so-called Born-Oppenheimer approximation for molecules) is the non-relativistic hamiltonian

$$\hat{H}_{\text{at}} = \sum_a \frac{\boldsymbol{p}_a^2}{2m} + \hat{V}, \tag{17}$$

where m is the electron's mass, $\boldsymbol{p}_a$ is the ath electron's momentum operator and $\hat{V}$ is the potential operator, describing interactions of electrons and atomic nuclei. Formally, if $|\Psi_i\rangle$ denote eigenstates of $\hat{H}_{\text{at}}$ with energies E_i, it can be written

$$\hat{H}_{\text{at}} = \sum_i E_i\,|\Psi_i\rangle\langle\Psi_i|\,. \tag{18}$$

Finally, $\hat{H}_{\text{int}}$ is the interaction hamiltonian, which can be derived from $\hat{H}_{\text{at}}$ through minimal coupling $\boldsymbol{p}_a \to \boldsymbol{\pi}_a = \boldsymbol{p}_a - e\boldsymbol{A}_a$, with $e < 0$ being the electron's charge and $\boldsymbol{A}_a \equiv \boldsymbol{A}(\boldsymbol{r}_a)$ denoting the vector potential in the ath electron's position. In vacuum,

$$\hat{H}_{\text{at}} + \hat{H}^{\text{vac}}_{\text{int}} = \sum_a \frac{\boldsymbol{\pi}_a^2}{2m} + \hat{V}. \tag{19}$$

The $\boldsymbol{A}_a^2$ term emerging from $\boldsymbol{\pi}_a^2$ does not (directly) contribute to spontaneous emission, because it contains no atomic operators and we neglect this term (what is in fact a usual procedure). Because $\left[r_a^i, p_b^j\right] = \mathrm{i}\hbar\delta_{ab}\delta^{ij}$, momentum $\boldsymbol{p}_a$ can be expressed as

$$p_a^i = \frac{m}{\mathrm{i}\hbar}\left[r_a^i, \hat{H}_{\text{at}}\right]. \tag{20}$$

We wish to concentrate on the interaction of electrons localized in a small volume near an atomic nucleus (or nuclei in case of a small molecule): this is the case for e.g. dopant atoms in solid state lasers, where emission is related to transition between two atomic levels. It is possible to study transitions of non-localized electrons, such as those in the conduction band of a bulk semiconductor (see e.g. [34]), but that is not the case here. Because optical wavelengths, which are of concern in light-emitting devices, are much longer than the radius of an atom, the interaction Hamiltonian can be simplified using the dipole approximation: $\boldsymbol{A}_a \approx \boldsymbol{A}(\boldsymbol{r}_0)$, where $\boldsymbol{r}_0$ is the position of the

system (understood as e.g. position of the center of mass). Then

$$\hat{H}_{\text{int}}^{\text{vac}} = \frac{\mathrm{i}}{\hbar} A^i(\boldsymbol{r}_0) \left[\mathrm{d}^i, \hat{H}_{\text{at}} \right], \tag{21}$$

where the electric dipole moment $\mathbf{d} = \sum_a e\boldsymbol{r}_a$. In dielectric media, the dipole moment interacts not with the macroscopic field, which is found as solution of Maxwell's equation, but with a microscopic local field [7]. This effect can be accounted for by inclusion of a field-enhancement factor $\mathcal{L}_{\text{diel}}$, usually defined as the ratio of local to macroscopic electric fields, but since the relation between the electric field and the vector potential is linear, it can be used with the vector potential as well. Thus, the interaction hamiltonian in a dielectric medium becomes

$$\hat{H}_{\text{int}} = \frac{\mathrm{i}}{\hbar} \mathcal{L}_{\text{diel}} A^i(\boldsymbol{r}_0) \left[\mathrm{d}^i, \hat{H}_{\text{at}} \right]. \tag{22}$$

At this point it is not necessary to define $\mathcal{L}_{\text{diel}}$ explicitly, and because its value depends on applied theory, we will proceed using only the general symbol. The interaction hamiltonian obtained in the derivation presented above is similar to the $\boldsymbol{E}\cdot\mathbf{d}$ form, but not equivalent. This form could be reconstructed if $\left[\mathbf{d}, \hat{H}_{\text{int}}\right] = 0$, because the commutator in (22) would denote the time derivative, which could be transferred onto the vector potential, turning it into an electric field. However, it is easy to check, that with the dipole approximation $\left[\mathbf{d}, \hat{H}_{\text{int}}\right] \approx -\mathrm{i}\hbar \frac{Ne^2}{m} \mathcal{L}_{\text{diel}} \boldsymbol{A}(\boldsymbol{r}_0)$, where N stands for the number of electrons. Hence, we use expression (22) for the interaction hamiltonian.

In dielectric media, vector-potential and electric-field operators obey the commutation rule [7]:

$$\left[A^i(\boldsymbol{r}), E^j(\boldsymbol{r}') \right] = -\frac{\mathrm{i}\hbar}{\varepsilon_0} \delta_{\varepsilon\perp}^{ij}(\boldsymbol{r}, \boldsymbol{r}') \tag{23}$$

and can be in the usual way expanded into effective resonator modes:

$$\boldsymbol{A}(\boldsymbol{r}) = \sum\!\!\!\!\!\!\int_{\boldsymbol{k},\epsilon} \sqrt{\frac{\hbar}{2\varepsilon_0 \omega_k}} \left(a_{k\epsilon} \boldsymbol{f}_{k\epsilon}(\boldsymbol{r}) + a_{k\epsilon}^\dagger \boldsymbol{f}_{k\epsilon}^*(\boldsymbol{r}) \right), \tag{24a}$$

$$\boldsymbol{E}(\boldsymbol{r}) = \mathrm{i} \sum\!\!\!\!\!\!\int_{\boldsymbol{k},\epsilon} \sqrt{\frac{\hbar\omega_k}{2\varepsilon_0}} \left(a_{k\epsilon} \boldsymbol{f}_{k\epsilon}(\boldsymbol{r}) - a_{k\epsilon}^\dagger \boldsymbol{f}_{k\epsilon}^*(\boldsymbol{r}) \right), \tag{24b}$$

where $a_{k\epsilon}$ and $a_{k\epsilon}^\dagger$ are the photon-annihilation and photon-creation operators, obeying the bosonic commutation rules:

$$[a_{k\epsilon}, a_{q\lambda}] = \left[a_{k\epsilon}^\dagger, a_{q\lambda}^\dagger \right] = 0, \tag{25a}$$

$$\left[a_{k\epsilon}, a_{q\lambda}^\dagger \right] = \delta_{\epsilon\lambda} \delta(\boldsymbol{k} - \boldsymbol{q}) \quad \text{(radiation and substrate modes)}, \tag{25b}$$

$$\left[a_{k_a\epsilon}, a_{q_b\lambda}^\dagger \right] = \delta_{\epsilon\lambda} \delta(k_x - q_x)\, \delta\left(k_y - q_y\right) \delta_{ab} \quad \text{(guided modes)}. \tag{25c}$$

The Hamiltonian of the electromagnetic field then obtains a form which is characteristic to an ensemble of harmonic oscillators:

$$\hat{H}_{\text{em}} = \sum\!\!\!\!\!\!\int_{\boldsymbol{k},\epsilon} \hbar\omega_k \hat{N}_{k\epsilon}, \tag{26}$$

where $\hat{N}_{k\epsilon} = a_{k\epsilon}^\dagger a_{k\epsilon}$ is the photon number operator with eigenvectors $|\ldots n_{k\epsilon} \ldots\rangle$, where $n_{k\epsilon} = 0, 1, 2, \ldots$ and:

$$a_{k\epsilon} |\ldots n_{k\epsilon} \ldots\rangle = \sqrt{n_{k\epsilon}}\, |\ldots (n_{k\epsilon} - 1) \ldots\rangle, \tag{27a}$$

$$a_{k\epsilon}^\dagger |\ldots n_{k\epsilon} \ldots\rangle = \sqrt{n_{k\epsilon} + 1}\, |\ldots (n_{k\epsilon} + 1) \ldots\rangle. \tag{27b}$$

4. Spontaneous emission

Spontaneous emission is a process in which a relaxing atom emits a single photon. Thus, for the description of this phenomenon, the Hilbert space of $\hat{H}_{\text{at}}$ can be restricted to only two eigenstates: $|\Psi_0\rangle$ and $|\Psi_1\rangle$ (we assume that $E_1 > E_0$), and the Hilbert space of $\hat{H}_{\text{em}}$ to eigenstates $|0\rangle$ – with no photons, and $|1_{k\epsilon}\rangle$ – with one photon in the mode with wave vector $\boldsymbol{k}$ and polarization ϵ. For the whole system, the excited state $|\Psi_1\rangle$ is accompanied by a state with no photons $|0\rangle$ and the lower state $|\Psi_0\rangle$ – by fields with one photon. The proper state vector is then:

$$|\psi(t)\rangle = C_0(t)\,|\Psi_1\rangle\,|0\rangle + \sum\!\!\!\!\!\!\int_{\boldsymbol{k},\epsilon} C_{k\epsilon}(t)\,|\Psi_0\rangle\,|1_{k\epsilon}\rangle\,. \tag{28}$$

The initial conditions adequate for spontaneous emission are:

$$C_0(t) = 1, \quad C_{k\epsilon}(t) = 0. \tag{29}$$

In the two-level case, states $|\Psi_0\rangle$ and $|\Psi_1\rangle$ can be chosen so that the transition dipole moment $\mathbf{d}_{10} = \langle\Psi_1|\,\mathbf{d}\,|\Psi_0\rangle \in \mathbb{R}^3$. In this paper we calculate the spontaneous-emission rate following the procedure described in [35]. After substitutions:

$$C_0(t) = b_0(t)\exp\left(-\frac{\mathrm{i}E_1 t}{\hbar}\right), \tag{30a}$$

$$C_{k\epsilon}(t) = b_{k\epsilon}(t)\exp\left(-\mathrm{i}\frac{\hbar\omega_k + E_0}{\hbar}t\right), \tag{30b}$$

where $b_0(t)$ and $b_{k\epsilon}(t)$ are probability amplitudes in the interaction picture the equations of motion become:

$$\frac{db_0}{dt} = \sum\!\!\!\!\!\!\int_{\boldsymbol{k},\epsilon} g_{k\epsilon} b_{k\epsilon}(t)\,\mathrm{e}^{\mathrm{i}(\Omega_{10}-\omega_k)t}, \tag{31a}$$

$$\frac{db_{k\epsilon}}{dt} = -\,g^*_{k\epsilon} b_0(t)\,\mathrm{e}^{\mathrm{i}(\omega_k-\Omega_{10})t}, \tag{31b}$$

where angular frequency of the atomic transition $\Omega_{10} = (E_1 - E_0)/\hbar$ and

$$g_{k\epsilon} = \frac{\langle 0|\,\langle\Psi_1|\,\hat{H}_{\text{int}}\,|\Psi_0\rangle\,|k\epsilon\rangle}{\mathrm{i}\hbar}. \tag{32}$$

In this case, if $\boldsymbol{r}_0$ denotes the position of the quantum system, then:

$$g_{k\epsilon} = -\frac{\mathcal{L}_{\text{diel}}\Omega_{10}\mathbf{d}_{10}\cdot\boldsymbol{f}_{k\epsilon}(\boldsymbol{r}_0)}{\sqrt{2\varepsilon_0\hbar\omega_k}}. \tag{33}$$

Symmetry of the multi-layer structure allows us to put $\boldsymbol{r}_0 = z_0\boldsymbol{e}_z$.
Formal solution of (31b) is:

$$b_{k\epsilon}(t) = -g^*_{k\epsilon}\int_0^t \mathrm{d}\tau\, b_0(\tau)\,\mathrm{e}^{\mathrm{i}(\omega_k-\Omega_{10})\tau}, \tag{34}$$

therefore:

$$\frac{db_0}{dt} = -\sum\!\!\!\!\!\!\int_{\boldsymbol{k},\epsilon} |g_{k\epsilon}|^2 \int_0^t \mathrm{d}\tau\, b_0(\tau)\,\mathrm{e}^{\mathrm{i}(\Omega_{10}-\omega_k)(t-\tau)}. \tag{35}$$

Assuming that b_0 varies slowly during the time interval from 0 to t, and putting it in front of the time integral (Markov process approximation) one obtains:

$$\frac{db_0}{dt} = -\sum\!\!\!\!\!\!\int_{\boldsymbol{k},\epsilon} |g_{k\epsilon}|^2\, b_0(t) \int_0^t \mathrm{d}\tau\,\mathrm{e}^{\mathrm{i}(\Omega_{10}-\omega_k)(t-\tau)}. \tag{36}$$

In the limit $t\to\infty$, the integral over τ becomes:

$$\lim_{t\to\infty}\int_0^t \mathrm{d}\tau\,\mathrm{e}^{\mathrm{i}(\Omega_{10}-\omega_k)(t-\tau)} = \pi\delta(\Omega_{10}-\omega_k) - \mathcal{P}\frac{\mathrm{i}}{\Omega_{10}-\omega_k}, \tag{37}$$

where $\mathcal{P}$ denotes the principal value. The term containing the delta function describes the decay process and can be used to determine the spontaneous emission rate, while the principal value term results in line shift $\delta\omega$, which is not of concern here. In the long time limit

$$\frac{db_0}{dt} = \left(-\frac{\Gamma}{2} + \mathrm{i}\delta\omega\right) b_0(t), \tag{38}$$

therefore

$$b_0(t) = \exp\left(-\frac{\Gamma t}{2}\right)\mathrm{e}^{\mathrm{i}\delta\omega t}, \tag{39}$$

where

$$\Gamma = \Gamma_{\text{RM}} + \Gamma_{\text{SM}} + \Gamma_{\text{GM}} \tag{40}$$

is the spontaneous emission rate. Contributions to Γ from different modes are therefore:

$$\Gamma_{\text{RM}} = 2\pi\sum_{\epsilon}\int_{\text{RM}} \mathrm{d}^3k\;|g_{k\epsilon}|^2\,\delta(\Omega_{10}-\omega_k), \tag{41a}$$

$$\Gamma_{\text{SM}} = 2\pi\sum_{\epsilon}\int_{\text{SM}} \mathrm{d}^3k\;|g_{k\epsilon}|^2\,\delta(\Omega_{10}-\omega_k), \tag{41b}$$

$$\Gamma_{\text{GM}} = 2\pi\sum_{\epsilon}\int \mathrm{d}^2k_{\parallel} \sum_{a\in\text{GM}(k_{\parallel},\epsilon)} \times\,|g_{k_a\epsilon}|^2\,\delta(\Omega_{10}-\omega_{k_a}). \tag{41c}$$

In the case of free space, the expression for Γ leads to the well-known Weisskopf-Wigner rate:

$$\Gamma^{\mathrm{fs}} = \frac{\mu_0 \Omega_{10}^3 \mathrm{d}_{10}^2}{3\pi\hbar c}. \tag{42}$$

With knowledge of b_0, solution of the equation of motion for $b_{k\epsilon}$ is:

$$b_{k\epsilon}(t) = g_{k\epsilon}^* \frac{1 - \exp\left(\mathrm{i}\left(\delta\omega + \omega_k - \Omega_{10}\right) t - \frac{\Gamma t}{2}\right)}{\mathrm{i}\left(\delta\omega + \omega_k - \Omega_{10}\right) - \frac{\Gamma}{2}}, \tag{43}$$

thus, in the limit $t \to \infty$:

$$\left|b_{k\epsilon}(t)\right|^2 = \frac{\left|g_{k\epsilon}\right|^2}{\left(\delta\omega + \omega_k - \Omega_{10}\right)^2 + \frac{\Gamma^2}{4}}. \tag{44}$$

5. Numerical calculations

The integration of $|g_{k\epsilon}|^2$ necessary to calculate the numerical value of Γ is best performed in spherical coordinates (k, ϑ, φ), where ϑ is the angle of incidence and φ is the azimuthal angle. Results of integration over φ can be obtained easily. Every $\boldsymbol{f}_{k\mathrm{TE}}$ lies within the xy plane and can be written in function of φ:

$$\boldsymbol{f}_{k\mathrm{TE}} = -P_k \boldsymbol{e}_x \sin\varphi + P_k \boldsymbol{e}_y \cos\varphi, \tag{45}$$

where

$$P_k = \boldsymbol{e}_y \cdot \boldsymbol{f}_{k\mathrm{TE}}\Big|_{\varphi=0}. \tag{46}$$

Because the structure has rotational symmetry, axes x and y can be chosen in in such a way that

$$\mathbf{d}_{10} = \mathrm{d}_\parallel \boldsymbol{e}_x + \mathrm{d}_z \boldsymbol{e}_z. \tag{47}$$

Then:

$$\int_0^{2\pi} \mathrm{d}\varphi \left|\mathbf{d}_{10} \cdot \boldsymbol{f}_{k\mathrm{TE}}\right|^2 = \pi \mathrm{d}_\parallel^2 \left|P_k\right|^2. \tag{48}$$

Every $\boldsymbol{f}_{k\mathrm{TM}}$ lies in the plane of incidence and can be written as a function of φ:

$$\boldsymbol{f}_{k\mathrm{TM}} = Q_{k\parallel} \boldsymbol{e}_x \cos\varphi + Q_{k\parallel} \boldsymbol{e}_y \sin\varphi + Q_{k\perp} \boldsymbol{e}_z, \tag{49}$$

with

$$Q_{k\parallel} = \boldsymbol{e}_x \cdot \boldsymbol{f}_{k\mathrm{TM}}\Big|_{\varphi=0} \tag{50a}$$

and

$$Q_{k\perp} = \boldsymbol{e}_z \cdot \boldsymbol{f}_{k\mathrm{TM}}. \tag{50b}$$

Then:

$$\int_0^{2\pi} \mathrm{d}\varphi \left|\mathbf{d}_{10} \cdot \boldsymbol{f}_{k\mathrm{TM}}\right|^2 = \pi \mathrm{d}_x^2 \left|Q_{k\parallel}\right|^2 + 2\pi \mathrm{d}_z^2 \left|Q_{k\perp}\right|^2. \tag{51}$$

Integration over ϑ has to be performed numerically.

5.1. Radiation modes

Radiation modes spread in the range of $0 \le \vartheta \le \vartheta_S$ and $\pi - \vartheta_S \le \vartheta \le \pi$, where

$$\vartheta_S = \arcsin \frac{\min\left\{n_{(0)}, n_{(L)}, n_{(R)}\right\}}{n_{(0)}}. \tag{52}$$

The contribution of the radiation modes Γ_{RM} to the spontaneous-emission rate is:

$$\Gamma_{\mathrm{RM}} = \frac{2\pi n_{(0)}^3 \Omega_{10}^2}{c^3} \sum_\epsilon \int_0^{\vartheta_S} \mathrm{d}\vartheta \sin\vartheta \int_0^{2\pi} \mathrm{d}\varphi \left[\left|g_{k\epsilon}\right|^2 + \left|g_{k_*\epsilon}\right|^2\right]_{k=n_{(0)}\Omega_{10}/c}. \tag{53}$$

In the second integral over φ it is possible to change the variable to $\varphi + \pi$ and obtain $|g_{-k\epsilon}|$ instead of $|g_{k_*\epsilon}|$. Then, because $|g_{-k\epsilon}| = |g_{k\epsilon}|$, using the known results of integration over φ after a few operations one arrives at

$$\Gamma_{\mathrm{RM}} = \frac{6\pi^3 n_{(0)}^3 \mathcal{L}_{\mathrm{diel}}^2 \Gamma^{\mathrm{fs}}}{\mathrm{d}_{10}^2} \int_{\eta_S}^1 \mathrm{d}\eta \left[\mathrm{d}_x^2 \left(\left|P_k\right|^2 + \left|Q_{k\parallel}\right|^2\right) + 2\mathrm{d}_z^2 \left|Q_{k\perp}\right|^2\right]_{\Theta=\Theta_{10}}, \tag{54}$$

with normalized transition frequency:

$$\Theta_{ij} = \frac{\Omega_{ij}}{2\pi f_0}, \tag{55}$$

$\eta_S = \cos\vartheta_S$ and

$$|P_k|^2 = \frac{\rho_{\mathrm{TE}}(\boldsymbol{k})}{n_{(0)}^2}\left(1 + \mathrm{Re}\left\{\xi_{\mathrm{TE}}(\boldsymbol{k})\,\mathrm{e}^{2\mathrm{i}k_z z_0}\right\}\right), \tag{56a}$$

$$\left|Q_{k\parallel}\right|^2 = \eta^2\frac{\rho_{\mathrm{TM}}(\boldsymbol{k})}{n_{(0)}^2}\left(1 - \mathrm{Re}\left\{\xi_{\mathrm{TM}}(\boldsymbol{k})\,\mathrm{e}^{2\mathrm{i}k_z z_0}\right\}\right), \tag{56b}$$

$$|Q_{k\perp}|^2 = \left(1-\eta^2\right)\frac{\rho_{\mathrm{TM}}(\boldsymbol{k})}{n_{(0)}^2}\left(1 + \mathrm{Re}\left\{\xi_{\mathrm{TM}}(\boldsymbol{k})\,\mathrm{e}^{2\mathrm{i}k_z z_0}\right\}\right). \tag{56c}$$

For radiation modes

$$\xi_\epsilon(\boldsymbol{k}) = \frac{r_R^*\left(1-|r_L|^2\right)\mathrm{e}^{-2\mathrm{i}k_z L_z} + r_L\left(1-|r_R|^2\right)}{1-|r_L r_R|^2}. \tag{57}$$

Coefficients (56) can easily be calculated using explicit definitions of field distributions from [29] or [31] (for more detail the reader is directed to reference [29] which includes explanations of all terms), knowing, that in those papers a few formulae for radiation modes can be significantly simplified, *i.e.*:

$$F_{k\epsilon} = \frac{n_{(0)}^2}{\rho_\epsilon(\boldsymbol{k})}, \tag{58a}$$

$$\tilde{F}_{k\epsilon} = \frac{n_{(0)}^2\xi_\epsilon^*(\boldsymbol{k})}{\rho_\epsilon(\boldsymbol{k})}, \tag{58b}$$

$$s_{k\epsilon} = \frac{1-\sqrt{1-|\xi_\epsilon(\boldsymbol{k})|^2}}{\xi_\epsilon(\boldsymbol{k})}. \tag{58c}$$

In free space, where all modes are of the radiation type, (54) correctly reproduces the Weisskopf-Wigner spontaneous emission rate, and in a multi-layer structure, contribution of each radiation mode is proportional to its mode spectrum.

5.2. Substrate modes

Substrate modes are found in the ranges of $\vartheta_S < \vartheta < \vartheta_G$ and $\pi - \vartheta_G < \vartheta < \pi - \vartheta_S$, where

$$\vartheta_G = \arcsin\frac{\min\left\{n_{(0)}, \max\left\{n_{(L)}, n_{(R)}\right\}\right\}}{n_{(0)}}. \tag{59}$$

However, these ranges contain the same modes [31], therefore they must not both enter into the integration. Thus, the contribution to the spontaneous-emission rate is given by:

$$\Gamma_{\mathrm{SM}} = \frac{3\pi^3 n_{(0)}^3\mathcal{L}_{\mathrm{diel}}^2\Gamma^{\mathrm{fs}}}{\mathrm{d}_{10}^2}\int_{\eta_G}^{\eta_S}\mathrm{d}\eta \times\left[\mathrm{d}_x^2\left(|P_k|^2 + \left|Q_{k\parallel}\right|^2\right) + 2\mathrm{d}_z^2\left|Q_{k\perp}\right|^2\right]_{\Theta=\Theta_{10}}, \tag{60}$$

where $\eta_G = \cos\vartheta_G$. For substrate modes:

$$|P_k|^2 = 2\frac{1+\mathrm{Re}\left\{\xi_{\mathrm{TE}}(\boldsymbol{k})\exp(2\mathrm{i}k_z z_0)\right\}}{F_{k\mathrm{TE}}}, \tag{61a}$$

$$\left|Q_{k\parallel}\right|^2 = 2\eta^2\frac{1-\mathrm{Re}\left\{\xi_{\mathrm{TM}}(\boldsymbol{k})\exp(2\mathrm{i}k_z z_0)\right\}}{F_{k\mathrm{TM}}}, \tag{61b}$$

$$|Q_{k\perp}|^2 = 2\left(1-\eta^2\right) \times\frac{1+\mathrm{Re}\left\{\xi_{\mathrm{TM}}(\boldsymbol{k})\exp(2\mathrm{i}k_z z_0)\right\}}{F_{k\mathrm{TM}}}, \tag{61c}$$

where $\xi_\epsilon(\boldsymbol{k}) = r_R^*\exp(-2\mathrm{i}k_z L_z)$, with the assumption that $n_{(R)} \le n_{(L)}$, and the coefficient $F_{k\epsilon}$ is given by (58a), just like in the case of the radiation modes, thus, these expressions are also proportional to the mode spectrum.

5.3. Guided modes

Guided modes occur at discrete angles ϑ_a from the range $\vartheta_G \le \vartheta_a \le \pi/2$ or $\pi/2 \le \vartheta_a \le \pi - \vartheta_G$. Just as in the case of substrate modes, guided modes with ϑ_a and $\pi - \vartheta_a$ (and the same polarization) are in fact the same mode, therefore summation has to be restricted to only one of these angles. Angles of incidence of guided modes are determined by the relation

$$\mathrm{e}^{\mathrm{i}\phi_a} \equiv r_R r_L \mathrm{e}^{2\mathrm{i}k_{z,a}L_z} = 1, \tag{62}$$

which allows us to find them as a function of frequency, or alternatively, their cosines as functions of normalized frequency $\eta_a(\Theta)$. Because

$$k_{z,a} = \frac{2\pi n_{(0)}\Theta\eta_a(\Theta)}{\Lambda}, \tag{63}$$

for a guided mode $|r_L| = |r_R| = 1$ and

$$\frac{d\phi_a}{d\Theta} = 0, \tag{64}$$

it is easy to find, that

$$\frac{d\eta_a}{d\Theta} = -\frac{\mathrm{Im}\left\{\frac{1}{r_L r_R}\frac{\partial}{\partial\Theta}(r_L r_R)\right\} + 4\pi\eta_a\frac{\Lambda^{(0)}}{\Lambda}}{\mathrm{Im}\left\{\frac{1}{r_L r_R}\frac{\partial}{\partial\eta}(r_L r_R)\right\} + 4\pi\Theta\frac{\Lambda^{(0)}}{\Lambda}}. \tag{65}$$

This equation can be solved numerically and allows to obtain values of η_a and its derivative for different Θ easier, than by solving (62) directly (with e.g. bisection method). Because

$$k_\parallel = \frac{2\pi n_{(0)}\Theta\sqrt{1-\eta_a^2(\Theta)}}{\Lambda} \tag{66}$$

integration over $\boldsymbol{k}_\parallel$ can be replaced by integration over Θ, which is carried out immediately, as

$$\delta(\Omega_{10} - \omega_{k_a}) = \frac{\delta(\Theta - \Theta_{10})}{2\pi f_0}, \tag{67}$$

and the guided modes' contribution to the spontaneous-emission rate turns out to be:

$$\Gamma_{\mathrm{GM}} = \frac{3\pi^2 n_{(0)}^2 \mathcal{L}_{\mathrm{diel}}^2 \Gamma^{\mathrm{fs}}}{2\Theta_{10}}\left[\sum_{a\in \mathrm{GM}_{\Theta,\mathrm{TE}}}\frac{\mathrm{d}_x^2}{\mathrm{d}_{10}^2}\Lambda\left|P_k\right|^2\left|1-\eta_{a,\mathrm{TE}}^2(\Theta)-\Theta\eta_{a,\mathrm{TE}}(\Theta)\frac{d\eta_{a,\mathrm{TE}}(\Theta)}{d\Theta}\right|\right.$$
$$\left. + \sum_{a\in \mathrm{GM}_{\Theta,\mathrm{TM}}}\frac{\mathrm{d}_x^2\Lambda\left|Q_{k\parallel}\right|^2 + 2\mathrm{d}_z^2\Lambda\left|Q_{k\perp}\right|^2}{\mathrm{d}_{10}^2}\left|1-\eta_{a,\mathrm{TM}}^2(\Theta)-\Theta\eta_{a,\mathrm{TM}}(\Theta)\frac{d\eta_{a,\mathrm{TM}}(\Theta)}{d\Theta}\right|\right]_{\Theta=\Theta_{10}}, \tag{68}$$

where $\mathrm{GM}_{\Theta,\epsilon}$ denotes the set of guided modes for normalized frequency Θ and polarization ϵ. For guided modes, P_k, $Q_{k\parallel}$ and $Q_{k\perp}$ are given by expressions of the same form as for the case of substrate modes. The relevant definition of $F_{k\epsilon}$ can be found in [30] or [31]. However, it is worth stressing that in the case of the guided modes, coefficients $F_{k\epsilon}$ have dimensions of length, thus ratios $F_{k\epsilon}/\Lambda$ are dimensionless. The term $\left|1-\eta_{a,\epsilon}^2(\Theta)-\Theta\eta_{a,\epsilon}(\Theta)\frac{d\eta_{a,\epsilon}(\Theta)}{d\Theta}\right|$ is often neglected, e.g. in [21]. It is, in fact, equal to unity in a resonator with metallic mirrors, but in a multi-layer structure the value can differ from this quite significantly.

6. Exemplary results

The expression derived in previous sections allows us to calculate and present numerical values of the spontaneous-emission rate, provided an explicit expression for $\mathcal{L}_{\mathrm{diel}}$ is specified. Following Glauber and Lewenstein [7], we put

$$\mathcal{L}_{\mathrm{diel}} = \frac{3n_{(0)}^2}{2n_{(0)}^2+1}, \tag{69}$$

which is the proper choice for substitutional impurities [36]. We have conducted calculations for the following structures:

- S1, with $\Lambda_1/\Lambda = 0.65$, $n_1 = 3$, $n_2 = 1.6$, $n_{(R)} = n_{(L)} = 1$ and $N_R = -N_L = 12$ (*i.e.* 6 periods in each direction starting from the $j = 0$ layer);
- S2, with $\Lambda_1/\Lambda = 0.5$, $n_1 = 1.4$, $n_2 = 1.2$, $n_{(R)} = 1$, $n_{(L)} = 1.1$ and $N_R = -N_L = 30$;
- S3, with $\Lambda_1/\Lambda = 0.5$, width defect in the $j = 0$ layer: $\Lambda^{(0)}/\Lambda = 0.7$, $n_1 = 1.4$, $n_2 = 1.2$, $n_{(R)} = 1$, $n_{(L)} = 1.1$ and $N_R = -N_L = 20$ (*i.e.* 10 periods in each direction starting the count from the $j = 0$ layer).

Results for structure S1 are presented in Fig. 2. The top plot contains the absolute values of reflection coefficients for stacks of layers on both sides of the $j = 0$ layer, calculated for $\eta = 1$, (*i.e.* perpendicular incidence). The middle plot contains the mode spectrum (normalized to the free-space value) for the same angle of incidence. These two plots show band gaps forming in the photonic crystal. Band gaps appear near the normalized frequency $\Theta_{\mathrm{B}} = 0.5$, corresponding to the Bragg wavelength $\lambda_{\mathrm{B}} = 2\Lambda$ and its multiplicities. For a band gap to form, a high quality factor of the cavity (layer) is required, therefore they appear in regions with high reflection, which are characterized by low values of the mode spectrum. In

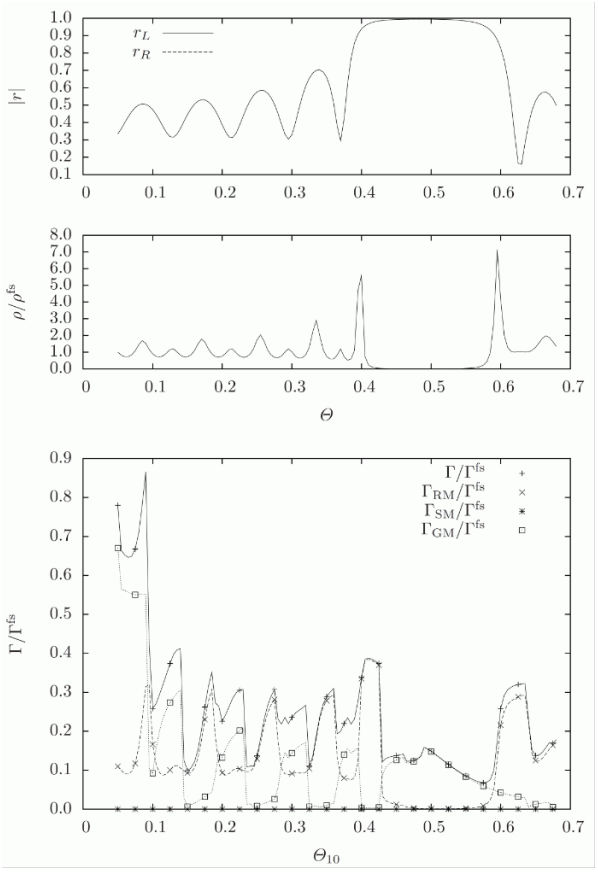

Figure 2. Absolute value of reflection coefficients, mode spectrum (both for $\eta = 1$) and spontaneous emission rates for structure S1.

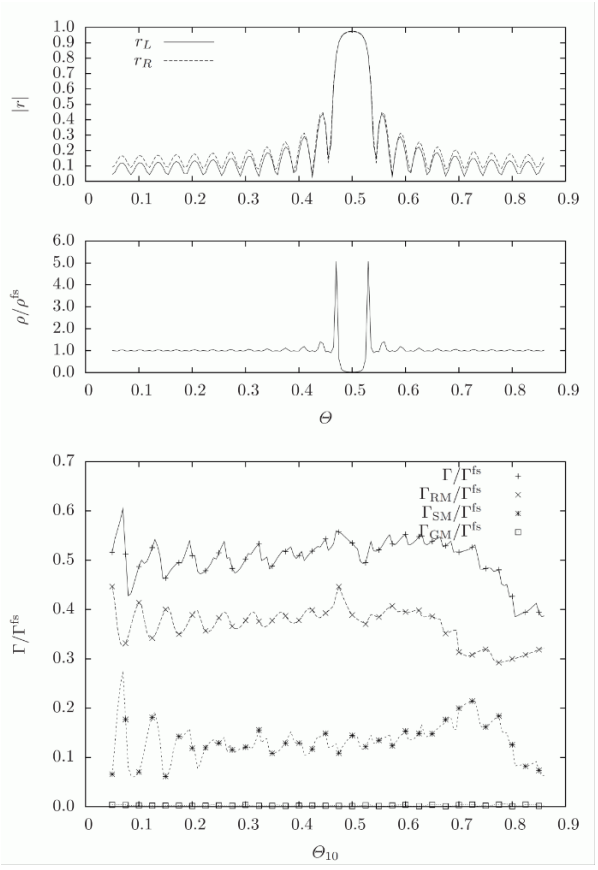

Figure 3. Absolute value of reflection coefficients, mode spectrum (both for $\eta = 1$) and spontaneous emission rates for structure S2.

a perfect photonic crystal, mode spectrum in a band gap would be equal to zero; in a real, finite structure this is not possible. The mode spectrum is high at the edges of a band gap, resembling an effect of the modes being "pushed out" of the bang gap. It is also possible to relate values of the mode spectrum to profiles of field distribution; for high value, the mode has a strong field in the layer, while for low values its field in the layer is weak. Because the emission rate is high for modes exhibiting strong fields at the location of the atom, modes with high mode spectra are expected to share most of the emitted power, while those with low mode spectra have negligible contributions to the overall rate. These observations allows us to interpret the bottom plot, showing the emission rate split into contributions from all mode types. For structure S1, the dielectric medium outside is the same so there are no substrate modes and $\Gamma_{SM} = 0$. The band gap for a lower η, seen in the middle plot, would slide towards higher Θ (because the k_z component of the wave vector is determined by λ_B), but in this structure, the band gaps for all η partially overlap, thus, it exhibits a full band gap. That is why a region of Θ in which the emission is practically forbidden is seen in the plot of the radiation modes' contribution Γ_{RM}/Γ^{fs}. A contribution from a few guided modes is present, however, meaning that for transition frequencies in the band gap the excitation of an atom would decay quite slowly with emission into these modes.

Similar results for structures S2 and S3 are plotted in Figs. 3 and 4. For these structures, n_1 and n_2 are too low for a full band gap to form, therefore they do not inhibit spontaneous emission as selectively as S1. Instead of trying to trace characteristic spots in Γ, which is roughly constant, it is much more interesting to investigate the contributions to the decay rate from modes with a given value of $\eta = 1$ (the same as those for which the mode spectrum was plotted), shown in Figs. 5 and 6. These plots make it evident, that there is a strict relation between the mode spectrum and contribution to decay rate, and therefore the probability of emission into a particular mode, given by (44), as well. It is also interesting to note

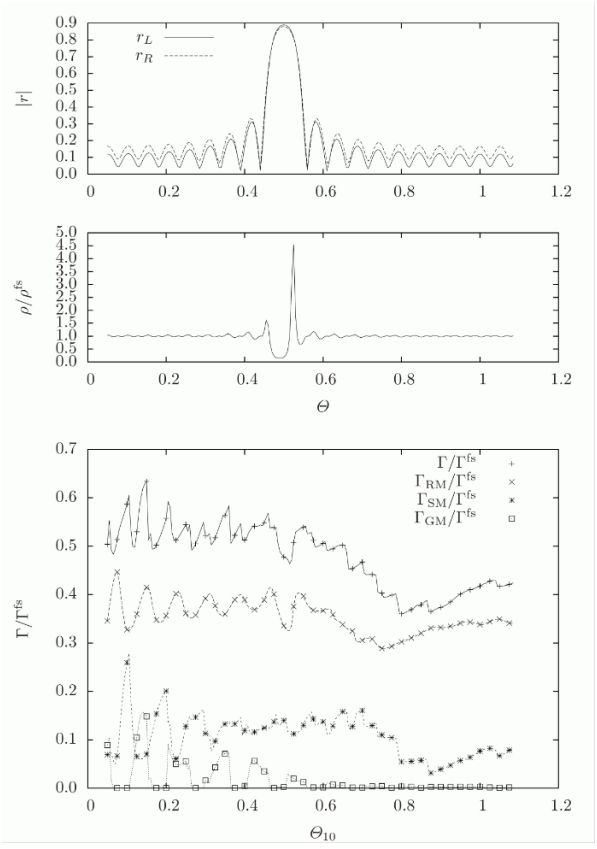

Figure 4. Absolute value of reflection coefficients, mode spectrum (both for $\eta = 1$) and spontaneous emission rates for structure S3.

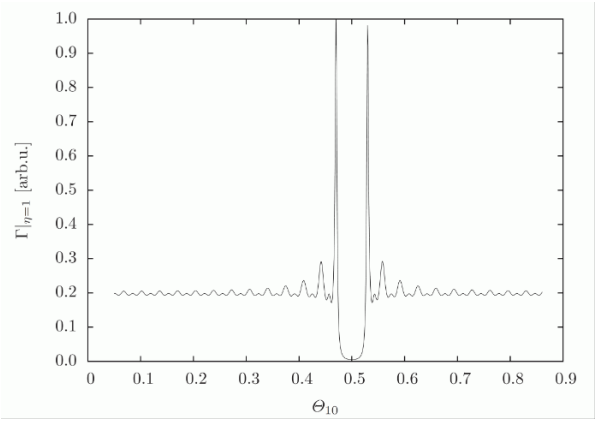

Figure 5. Contribution to Γ at $\eta = 1$ for structure S2.

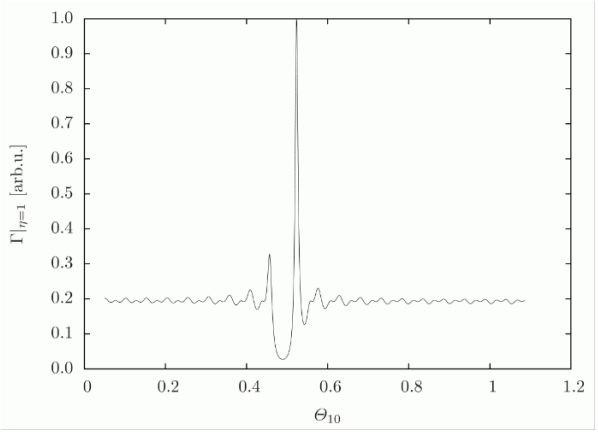

Figure 6. Contribution to Γ at $\eta = 1$ for structure S3.

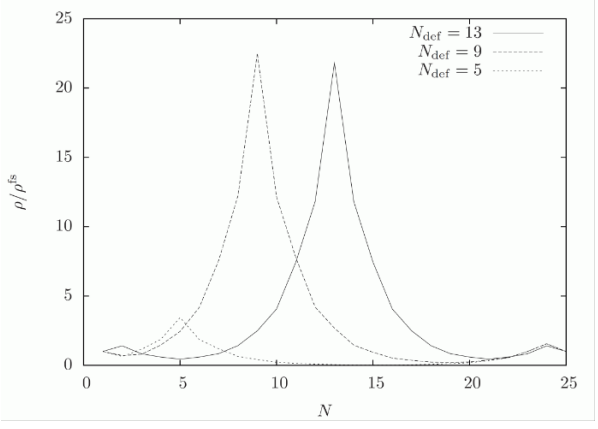

Figure 7. Mode spectrum of a defect mode in consecutive n_1 layers of photonic crystal S1 with a defect introduced in layer N_{def} (for $\eta = 1$, N stands for the index of elementary cell).

that the defect of structure S3, which results in a defect mode seen in the mode spectrum inside the band gap, does not increase the total decay rate, but it rather helps to direct the emission into specific modes. At each frequency defect modes occur only at one angle of incidence, while maxima at the edges of the band gap can appear at two, thus, structure S3 makes a better control of the emission, than S2.

The characteristic emission rate for an atom in a specific layer is proportional to the mode spectrum in that layer, therefore analysis of the variation of the mode spectrum in different layers reveals important information about the structure. One of the most interesting results is presented in Fig. 7. In this figure, the mode spectrum of a defect mode in n_1 layers of different elementary cells of structure S1 with a defect introduced in one of its layers is plotted. It is clearly seen that the defected layer is characterized by the maximal value of the mode spectrum, which quickly becomes much smaller in surrounding layers. The maximal value depends also on the situation of the defected layer. It follows from the obtained expressions that the

same is the behaviour of the spontaneous-emission rate into the defect mode. Similarly, in case of a 1D photonic crystal with multiple defects (analyzed in [32]), the results presented therein can be immediately related to the spontaneous-emission rate. This conclusion could not have been drawn from the density of states calculated for the whole structure or with a model assuming external excitation and is a good example of one of the effective resonator model's advantages.

7. Summary

In this paper we have obtained expressions describing spontaneous emission rates in a structure of finite one-dimensional photonic crystal with arbitrary defects. Our derivation has been based on the effective resonator model, which allows us to calculate field distributions and defines a quantity called the mode spectrum, which contains information about the physical properties of a particular layer of the structure. Thanks to this property, the mode spectrum is much more useful for analyzing the structure's properties than, for example, density of states, characterizing the whole structure, because it allows easy observation of effects associated with different parts of the structure. We have defined a set of dimensionless structural parameters, which are very convenient to work with, in particular the derived formulae for the spontaneous-emission decay rate are fully expressed. We have discussed contributions from modes of different types, and shown that contributions from radiation and substrate modes are proportional to the mode spectrum. This is an important result, because calculation of the mode spectrum is much easier than that of the field distribution, and provides an easy way to investigate how structure affects the emission of electromagnetic radiation. Employing the mode spectrum for an analysis is particularly beneficial in the case of defected structures, allowing easy revelation of defect modes or their behaviour throughout the structure, what is not always easy to accomplish with other models. Exemplary results included in the text indicate that the developed description can easily characterize spontaneous emission from a defected layer or any nearby layer, and also provides information on how localization of a field changes when the defected layer is moved in the photonic crystal. Thus, we have shown that the effective resonator model is a suitable tool for modeling spontaneous emission from multi-layer structures, including defected finite one-dimensional photonic crystals, which can be easily applied in various practical designs.

Acknowledgements

This work has been financially supported by State Committee for Scientific Research, project N N515 052535.

References

[1] Z. Białynicka-Birula, Acta Phys. Pol. B 27, 2409 (1996)
[2] E. M. Purcell, Phys. Rev. 69, 681 (1946)
[3] P. Goy, J. M. Raimond, M. Gross, S. Haroche, Phys. Rev. Lett. 50, 1903 (1983)
[4] F. de Martini, M. Marrocco, P. Mataloni, L. Crescentini, R. Loudon, Phys. Rev. A 43, 2480 (1991)
[5] K. Nishioka, K. Tanaka, T. Nakamura, Y. Lee, M. Yamanishi, Appl. Phys. Lett. 63, 2944 (1993)
[6] M. D. Tocci, M. Scalora, M. J. Bloemer, J. P. Dowling, Ch. M. Bowden, Phys. Rev. A 53, 2799 (1996)
[7] R. J. Glauber, M. Lewenstein, Phys. Rev. A 43, 467 (1991)
[8] J. W. Strutt (Lord Rayleigh), Philos. Mag. 24, 145 (1887)
[9] J. N. Winn, Y. Fink, S. Fan, J. D. Joannopoulos, Opt. Lett. 23, 1573 (1998)
[10] D. N. Chigrin, A. V. Lavrinenko, D. A. Yarotsky, S. V. Gaponenko, Appl. Phys. A 68, 25 (1999)
[11] H.-Y. Lee, T. Yao, J. Appl. Phys. 93, 819 (2003)
[12] S. Bastonero et al., Opt. Quant. Electron. 31, 857 (1999)
[13] M. Bugajski, J. Muszalski, T. Ochalski, J. Kątcki, B. Mroziewicz, Acta Phys. Pol. A 101, 105 (2002)
[14] A. S. Sánchez, P. Halevi, Phys. Rev. E 72, 56609 (2005)
[15] W. Lukosz, Phys. Rev. B 22, 3030 (1980)
[16] C. K. Carniglia, L. Mandel, Phys. Rev. D 3, 280 (1971)
[17] H. Hammer, J. Mod. Optic. 50, 207 (2003)
[18] I. Białynicki-Birula, J. B. Brojan, Phys. Rev. D 5, 485 (1972)
[19] W. Żakowicz, Acta Phys. Pol. A 101, 119 (2002)
[20] C. Creatore, L. C. Andreani, Phys. Rev. A 78, 063825 (2008)
[21] H. Rigneault, S. Monneret, Phys. Rev. A 54, 2356 (1996)
[22] Z. H. Wang, Opt. Commun. 144, 187 (1997)
[23] P. Yeh, A. Yariv, C.-S. Hong, J. Opt. Soc. Am. 67, 423 (1977)
[24] P. Yeh, Optical waves in layered media (John Wiley & Sons, New York, 1988)
[25] H. Benisty, H. de Neve, C. Weisbuch, IEEE J. Quantum Elect. 34, 1612 (1998)
[26] J. Muszalski, Semiconductor Microcavities (ITE,

Warszawa, Poland, 2002)
[27] A. Rudziński, A. Tyszka-Zawadzka, P. Szczepański, Proc. SPIE 5950, 59501A (2005)
[28] A. Rudziński, Acta Phys. Pol. A 111, 323 (2007)
[29] A. Rudziński, Acta Phys. Pol. A 112, 495 (2007); erratum: Acta Phys. Pol. A 112, 1327 (2007)
[30] A. Rudziński, Acta Phys. Pol. A 112, 505 (2007); erratum: Acta Phys. Pol. A 113, 1709 (2008)
[31] A. Rudziński, Acta Phys. Pol. A 115, 660 (2009)
[32] A. Rudziński, A. Tyszka-Zawadzka, P. Szczepański, Opt. Quant. Electron. 39, 501 (2007)
[33] A. Rudziński, P. Szczepański, In: IEEE Eurocon 2007, 9-12 Sep. 2007, Warszawa, Poland
[34] Ch. Hooijer, G. Li, K. Allaart, D. Lenstra, IEEE J. Quantum Elect. 37, 1161 (2001)
[35] P. Meystre, M. Sargent, Elements of Quantum Optics (Springer-Verlag, Berlin, 1991)
[36] P. de Vries, A. Lagendijk, Phys. Rev. Lett. 81, 1381 (1998)